Investigative studies on performance characteristics of aerodynamic foil thrust bearings with various foil configurations

S. Supreeth[1] · T. N. Raju[2] · R. N. Ravikumar[3]

Abstract

Foil thrust bearings (FTB) used in low-power gas turbines are self-acting (aerodynamic) bearings that sustain high-speed shafts under lightly loaded conditions with air (fluid) as the lubricant. The present research deals with the enhancement of load capabilities of the Air Foil Thrust Bearing (AFTB) operating under hydrodynamic condition by conducting experiments on a newly developed instrumented bearing test rig catering to speeds up to 20,000 rpm. The parametric and quantitative experimental research comprises of design, fabrication, and testing of various top foil configurations of gas lubricated FTB (larger diameter of about 224 mm) at atmospheric conditions. Numerous combinations of air foil bearings with heat-treated steel and copper foils are examined both statically and dynamically in obtaining the best possible AFTB with optimum foil stiffness. The foil geometric parameters namely foil thickness and sector angle of the foils are varied for both materials that affected the performance of an AFTB in terms of load carrying capabilities. The current investigative studies on FTB as a function of pre-load constitutes data such as structural stiffness, axial load, frictional torque, power loss, and lubricant temperature.

Keywords Air foil thrust bearing · Axial loads · Foil configuration · Angular foils · Structural stiffness · Frictional torque

1 Introduction

Foil thrust bearings (FTB) are physically non-contact self-acting hydrodynamic bearings that sustain lightly loaded, high-speed shafts in hostile conditions by employing process fluid (usually air) as the medium of operation. While the foil offers damping and stiffness, the gas that is present between the high-speed runner and the foil serves as a lubricating medium and sustains the axial load at high speed owing to the formation of an air wedge layer. Accurate manufacturing with optimised foil design of aerodynamic foil thrust bearings (AFTB) are essential for their effective performance at greater speeds in order to achieve the appropriate load carrying capabilities. Significant advantages of these bearings in high-speed turbo machineries include lightweight, high reliability, contaminant-free circumstances, elevated temperature operation, and complete use of lubrication. Over the last three decades, a variety of devices such as cryogenic turbo expanders, micro turbine generators, turbo blowers, air cycle machines (ACM), and air cycle refrigeration units, have relied on these gas foil thrust bearings (GFTB).

Earlier input on radial and dual spring thrust foil bearings by Giri Agarwal [1] and foregoing technologies of compliant foil bearings discussed by Heshmat H [2] were a part of substantial research on AFTB. The major factors influencing the performance of the foil thrust bearing in terms of load carrying capabilities were discussed briefly by Supreeth et al. [3] where the foil thickness and foil geometry had a significant role. Preliminary research by Yong Bok Lee et al. [4] on three bump air thrust foil bearings (AFTB) with outer diameters of 110 mm, 100 mm, and 90 mm for axial loads at rotational speeds from 10,000 rpm to 25,000 rpm

✉ S. Supreeth
  supreeth.s1994@gmail.com

1 Department of Mechanical Engineering, East West Institute of Technology (affiliated to Visvesvaraya Technological University (VTU), Belagavi), Bangalore 560091, India

2 Department of Mechanical Engineering, Dr. Ambedkar Institute of Technology (affiliated to Visvesvaraya Technological University (VTU), Belagavi), Bangalore 560056, India

3 Department of Mechanical Engineering, BMS College of Engineering (affiliated to Visvesvaraya Technological University (VTU), Belagavi), Bangalore 560019, India

revealed that larger diameter bearings carried higher loads at elevated speeds. Fibonacci grove FTB of 29 mm diameter developed by Hyuga Kikuchi et al. [5] had enhanced performance in terms of load, temperature, and friction tested up to 30,000 rpm. Tae Ho Kim and others [6] briefly studied on the tilting angles of GFTB that had decrease in load capacity of the GFTB operated at 30,000 rpm, while another research study by Yong Bok Lee et al. [7] focused on the power losses of the FTB placed in-between a compressor and a turbine operated up to 1,36,000 rpm. Static studies by Ting Shi and others [8] enlightened on the stiffness, displacement, and thrust load for about nine different foil configurations of the thrust foil bearings. Temperature studies on FTB (64 mm bearing diameter) by placing k-type thermocouples underneath the foils for determining the bearing characteristics was demonstrated by Xiaomin Liu et al. [9]. Yu Guo and other researchers [10] made significant contribution by introducing cooling air that reduces the bearing temperature at high speeds with no change in pre-load and operating speeds of a multi-leaf FTB. Thrust foil bearing with four 90^{0} sector angled beryllium bronze foils with hemispheric convex dotted foils were used as bottom foils, as tested by R. G. Chen and others [11].

Viscoelastic supported hydrodynamic FTB with four top foils (beryllium bronze) and a bottom foil (fluorine rubber foil) carried higher loads for 1 lakh rpm operating speeds (diameter 38 mm) was developed by Zhou et al. [12]. Brain Dykas and others [13] designed, fabricated, and tested a prototype of a thrust foil bearing using Inconel X-750 (for the bump and top foils) with 45^{0} sector angle and bump foils of five strips mounted on a 100 mm diameter bearing pad. Kozanecki et al. [14] conducted experimentation on GFTB on a test bench that measured the speed and frictional torque where they noticed a decrease in frictional torque with an increase in operating speed (up to 24,000 rpm) over a time period, with a constant load applied to the said bearing. Variation of drag torque with static load for operating speed up to 80,000 rpm were demonstrated by Xu and others [15] for an AFTB (72 mm foil diameter) having four different foil thickness on a newly developed test rig employed by a high speed motor. The foil deflections and thrust loads at dynamic condition (21,000 rpm) measured by Changlin Li et al. [16] for a multi-layered FTB on a test rig were in consistent with the theoretical model. Recent experimental studies on FTB with 60 mm diameter by Ravikumar et al. [17] with a single top layer operated up to 45,000 rpm were validated with COMSOL results. Research on AFTB with multilayer or cascaded foils were conceptualised by them [18] for 0.1 mm, 0.2 mm, and 0.3 mm foil thicknesses. Parametric studies by Supreeth and others [19] optimised the foil stiffness by varying the number of foils, foil thickness, and foil gap on a novel bearing test rig and they [20] also provided a bearing dimensionless number that emphasises the various

performance factors of the oil-free FTB. Sung Hwang and their team [21] conducted experiments on FTB (dia. 61 mm) with a varying top foil inclination angle subjected to constant static loads at different operating speeds and revealed that increase in preload increases the drag torque. The fluid-thermal-structure interaction (FTSI) of a GFTB with four bump foil configuration operated at 30,000 rpm were validated for dynamic load capacity with that of experimentation by Bin Hu et al. [22].

Although air foil bearings are nowadays widely being used in turbocharges that have applications in aircraft engines, marine engines and in numerous locomotives according to Tammineni et al. [23], research on air/gas lubricated FTB that could withstand larger loads are of great essential. Despite significant advancements in the research and development of foil thrust bearings, several research gaps and challenges remains to be addressed such as optimization of design (geometric) and stiffness parameters, understanding of performance under numerous operating conditions, development of advanced foil materials, etc. Present study deals with design, building, and testing of gas lubricated FTB having larger diameter (224 mm) for about sixteen different foil arrangements on a newly developed bearing test rig catering to speeds up to 20,000 rpm. Fabrication of foils, thrust pad, and runner instituted in this paper minimises the total mass and cost including the production techniques with the easily available foil material. Based on various literatures, numerous scientists and researchers have examined AFTB by considering the top foil with bump foil and or viscoelastic supports, however this research study primarily concentrates on GFTB without bump foil that eliminates the design and fabrication complexity. Owing to the significance that foil stiffness played on bearing loads, it becomes apparent that altering or varying the stiffness of a single top foil was sufficient in providing adequate thrust loads. The performance of the proposed non-contact FTB prototype in terms of load carrying capabilities are evaluated experimentally among the numerous foil arrangements, that is best suited to operate a turbocharger used in food processing industries.

2 Experimental study

The novel bearing test rig developed in the present study is illustrated in Fig. 1 comprises of a horizontal testing section mounted on a well-built concrete base with a strong damping. The instrumented AFTB testing rig is a metal base plate table top testing apparatus (as pictured in Fig. 2) with a drive unit has a high speed spindle that is driven by a high speed motor by means of a belt drive, consuming a three phase power of 6 kW. The aluminium thrust runner of 224 mm diameter with 10 mm thickness is mounted on

Fig. 1 Illustration of the FTB test rig
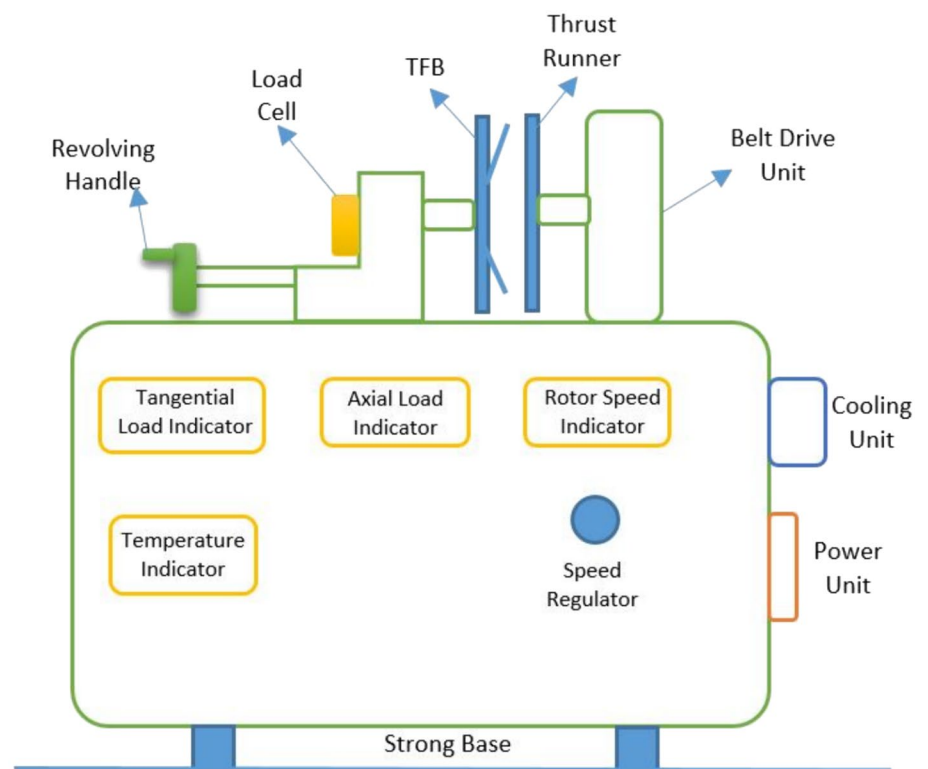
Fig. 2 Picture of the bearing testing apparatus

this rotating spindle which is cooled by a separate cooling unit with a distilled water to prevent the rise in temperature. Proximity sensor is used in measuring the rotations of the thrust runner or the rotating disc that is placed behind the spindle and the speed in terms of rpm is displayed on the rotor speed indicator. Variable frequency drive (VFD) or the speed regulator controls the speed rate of the drive operated manually by means of a rotary knob. The aluminium bearing pad or backing plate having a diameter of 224 mm and 10 mm width with a surface contact area of 36,191 mm^2, has twelve thin slots with small holes for the attachment of foils as shown in Fig. 3. Thin metallic foils of uncoated pure copper ($E = 130,000$ N/mm^2) and SS304 grade steel ($E = 193,000$ N/mm^2) with 0.3 mm and 0.4 mm thicknesses are the two available materials used in the present study. Laser cutting technology and computer numeric control (CNC) bending were employed in profile cutting of the foils for four types of sector angle or SA (namely 45°, 60°, 75°, and 90°) for both thicknesses and for both materials. The ramp angle or the foil inclination angle (IA) is kept constant for all the foil profiles (i.e., $\alpha = 15°$) as sketched in Fig. 3. All the copper and steel foils are heat treated (Fig. 4) separately for relieving of residual stresses that are due to bending and to enhance their strength and ductility. These angular foils with various desirable foil configurations are fixed on the blackened backing pad with fasteners for easy removal.

The bearing pad with foils termed as foil thrust bearing (FTB) assembly is placed exactly parallel to the thrust runner on a sliding pedestal that moves horizontally along the axis of the rotating spindle. The displacement of the pedestal unit towards the runner is controlled by means of a revolving handle (as pictured in Fig. 5). Button type load cell is placed on the sliding pedestal that measures the axial load of the FTB assembly in terms of newtons (N) and is displayed
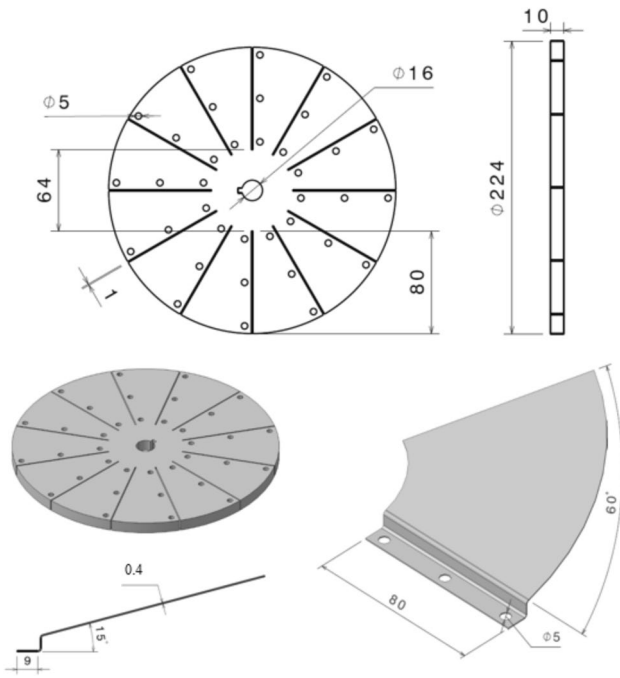
Fig. 3 Geometrical drawings of the bearing pad and the foil (all dimensions in mm)

Fig. 4 Heat treated 75° steel foil and 45° copper foil of 0.4 mm thickness

on the control panel. The rotational (frictional) movement of the mounted foil bearing pad is restricted by means of a small lever that rests on a load cell tangentially. This tangential cum frictional load in terms of newtons (N) is shown on the control panel of the bearing apparatus. Four thin k-type thermocouples are placed in-between the bearing plate and the foils in opposite direction that measures the temperature of the surrounding air which is displayed in Celsius scale (°C). AFTB for about sixteen different foil arrangements with eight copper foil configurations and eight steel foil configurations are presented in current work. FTB with bearing configuration numbers BS1 to BS8 representing steel foil arrangements are as tabulated in Table 1. Similarly
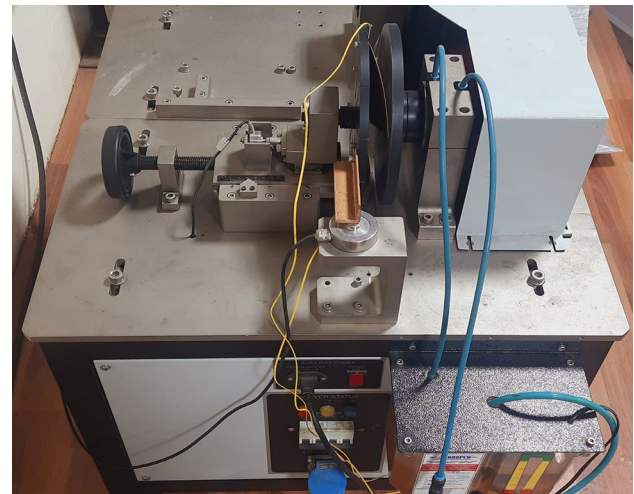

Fig. 5 Side view of the AFTB test rig

Table 1 AFTB with steel foil configurations

Sl. no.	Bearing configuration no	Thickness of the foil	Sector angle of the foil	Number of foils
1	BS1	0.3 mm	45°	08
2	BS2	0.3 mm	60°	06
3	BS3	0.3 mm	75°	04
4	BS4	0.3 mm	90°	04
5	BS5	0.4 mm	45°	08
6	BS6	0.4 mm	60°	06
7	BS7	0.4 mm	75°	04
8	BS8	0.4 mm	90°	04

Table 2 AFTB with copper foil configurations

Sl. no.	Bearing configuration no	Thickness of the foil	Sector angle of the foil	Number of foils
1	BC1	0.3 mm	45°	08
2	BC2	0.3 mm	60°	06
3	BC3	0.3 mm	75°	04
4	BC4	0.3 mm	90°	04
5	BC5	0.4 mm	45°	08
6	BC6	0.4 mm	60°	06
7	BC7	0.4 mm	75°	04
8	BC8	0.4 mm	90°	04

BC1 to BC8 indicates copper foil configuration numbers tabulated in Table 2 corresponds to FTB with copper foil arrangements. The maximum number of angular foils that could be attached on a bearing pad is limited based on the

circumference angle i.e., 360° (hence four 90° foils, four 75° foils, six 60° foils, and eight 45° foils are accommodated for both 0.3 mm and 0.4 mm thicknesses of copper and steel foils), however more number of foils on the bearing pad overlap with each other. Each time the required set of foils as per the desired foil configurations are fixed on the backing plate and then mounted on the pedestal for experimentation and other calculations. Two post-tested GFTB with four sets of 0.3 mm 60° SA steel foils and 45° SA copper foils are as pictured in Fig. 6.

3 Discussions on results

The present research endeavours an exhaustive series of experiments, meticulously covering all potential combinations of foil thrust bearings as delineated in Tables 1, 2. These comprehensive trials were conducted within a controlled test rig environment, scrutinizing the bearings performance under both static and dynamic conditions. To maintain a pragmatic and readily accessible approach, two readily accessible foil materials, namely steel and copper were chosen for the current investigation even though material characteristics does not affect the bearing load performance, with the exception of surface roughness. It is important to note that the larger bearing diameters necessitated thicker foils to withstand axial loads with minimal deflection and conversely greater stiffness was achieved by opting thicker foils (especially when dealing with bearings having larger cross-sectional area). The experimental procedure was executed meticulously, with a keen focus on evaluating the performance of various FTB combinations under atmospheric conditions. The ensuing section delves into a comprehensive discussion of the experimental methodology and intricacies of the results of the bearing garnered from three extensive trials.
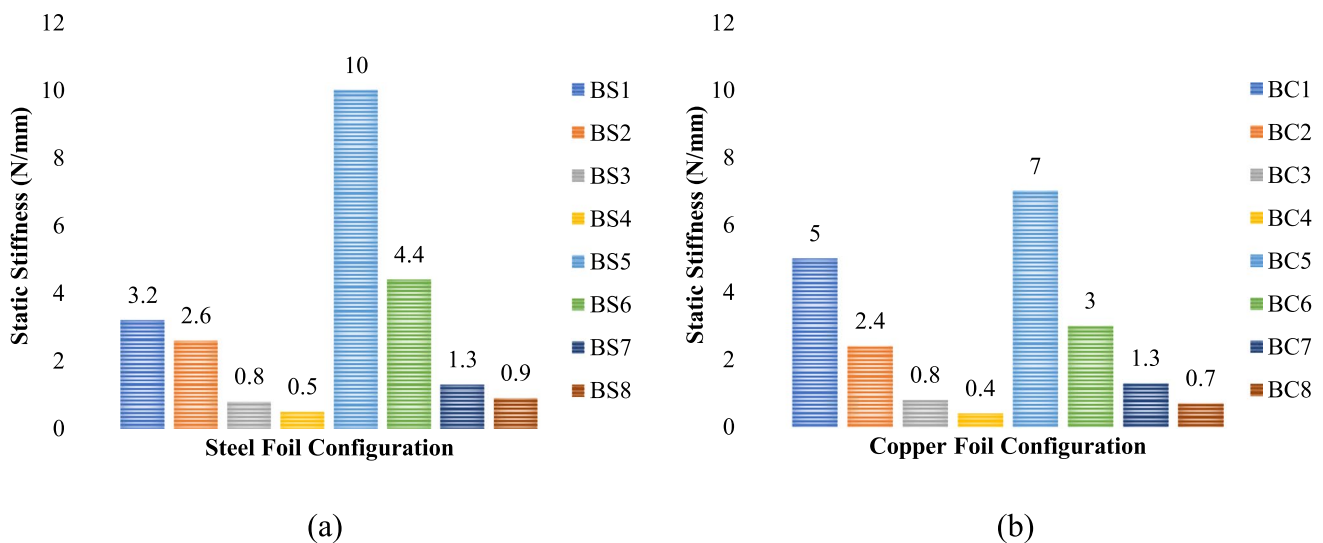
3.1 Structural stiffness

The bearing unit with BS1 foil arrangement is placed on the pedestal of the bearing testing apparatus using a keyway to restrict the motion in all directions of the FTB. To align the foils with the runner in parallel, the pedestal is manually altered using a revolving handle. However, there is a discrepancy in the height between the outer edge (OE) and the inner edge (IE) of the foil concerning the thrust runner or the backing plate surface (i.e., OE ≠ IE). As soon as all the foils make contact with the thrust runner, an axial load will be applied which is digitally displayed on the apparatus, and the bearing assembly being continuously moved towards the runner as long as the heights of OE and IE become equal and parallel (i.e., OE = IE) imposing a maximum pre-load. At this juncture, the gap between the bearing assembly and the thrust runner is nearly the same (about 5 mm) for all foil combinations, whereas the applied pre-load varies for foils with different sector-angles.

The deflection or deformation of the foils due to the applied pre-load are measured based on the pedestal displacement that is noted by means of a measurement scale placed on sliding bed of the apparatus. This load by deflection ratio gives the static structural stiffness for a GFTB with 0.3 mm eight steel foils with 45° sector angle (BS1), which is about 3.2 N/mm. This procedure is repeated for other steel foil combinations (BS2 to BS8), and the static structural stiffness is plotted in Fig. 7a. For each measurement, the bearing assembly with the necessary set of foils is placed parallel against the thrust runner on the sliding pedestal. The results indicate that the FTB with a BS5 foil configuration exhibits higher stiffness compared to all other thrust foil bearing combinations, approximately 10 N/mm. Corresponding static test results for GFTB with copper foil combinations (BC1 to BC8) are shown in Fig. 7b, and the measured structural stiffness is higher for BC5 foil combination. However, the stiffness characteristics of GFTB with

Fig. 6 Photographs of post-tested GFTB with four **a** 60° steel foils and **b** 45° copper foils

(a)   (b)
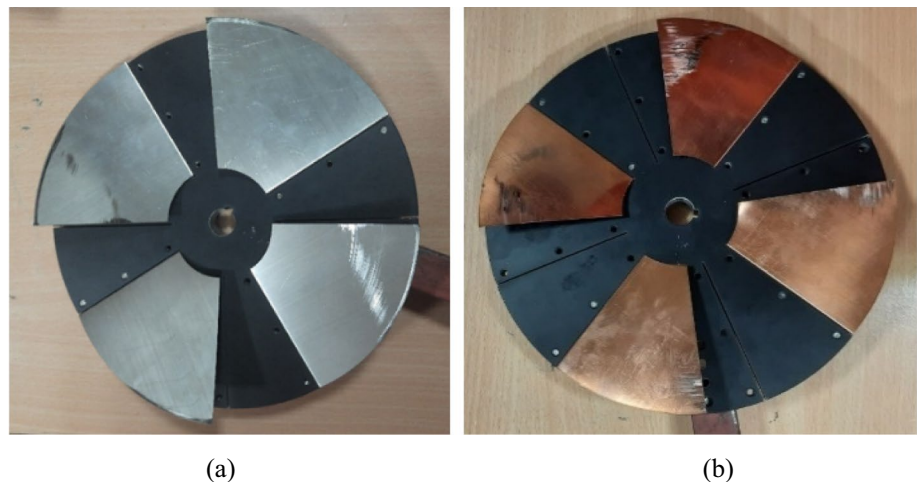
Fig. 7 Static structural stiffness of GFTB with steel and copper foil configurations

copper foils behave similarly to that of steel foils, while the FTB with steel foils possess greater stiffness for a given or constant foil geometry when compared to copper foils.

3.2 Thrust loads

For all the GFTB foil combinations, the greatest possible axial loads are determined under dynamic conditions with runner speeds ranging between 10,000 rpm and 20,000 rpm. Initially, the bearing assembly with various foil combinations (BS1 to BS8 in case of steel foils and BC1 to BC8 in case of copper foils) with a maximal preload and OE = IE is preserved as in the case of static condition. By controlling the VFD manually, the spindle or the thrust runner is rotated in counter-clockwise direction for desirable speeds. At first, the foils rubs (makes contact) against the runner surface until the rotor achieves higher speeds subsequently a wedge film region is formed by the deflection of foils, due to which the pressurized fluid film carries the thrust load. The obtained dynamic loads recorded from the bearing test rig indicator represents the maximum axial forces applied on all the foils for all the corresponding rotating speeds. The wear on the top surface of all the foils under dynamic tests due to start-stop cycles (as pictured in Fig. 6) is typical until the lift-off speed which occurs roughly at approximately 4500 rpm. The thrust load values for an AFTB, configured with both steel and copper foils are plotted against the operating speeds as plotted in Figs. 8, 9.

From the graph it is evident that AFTB with BS5 foil configuration supported higher loads than that of all other foil combinations. All of these bearings' load capacities increased (though not linearly) with higher rotating speeds while each foil configuration has a unique peak load-bearing ability in relation to various operating speeds, i.e., at higher speeds the foils deflect more quickly and become less stiff from carrying heavier loads (which is due to larger fluid pressure and thicker fluid film). The static stiffnesses and dynamic loads of AFTB with BS5 and BS6 were higher due to larger number of foils with greater thickness and smaller sector angles. Similar experimental studies on FTB with copper foils manifested the maximum load being supported by BS5 foil configuration as in case of steel foils. Sincere attempts were made to test the thrust foil bearing using 0.5 mm thick steel and copper foils, but no load could be drawn owing to either the high foil stiffness resulting from an increase in foil thickness or the relatively low operating speeds (fluid pressure) which were insufficient to deflect the foils. It was observed that when rotational speeds of an AFTB rise, so does the bearing's capacity to support loads concerning to various heat treated foil combinations. Nevertheless it was found that the optimal foil stiffness (with respect to foil geometry), foil thickness, and operational speeds yield the maximum thrust load of an AFTB.

The aerodynamic thrust foil bearings with BC1, BC5, BS1, and BS5 foil configurations consisted of eight number of circumferential foils as tested for both static and dynamic cases. However, the bearing pad assembly with two foils, four foils, six foils, and eight foils for all these mentioned foil configurations were tested to record the dynamic thrust loads (as plotted in Fig. 10). It was found that the load capability of the FTB increased linearly with the increase in number of foils for BC1 (45° SA copper foil with 0.3 mm thickness), BC5 (45° SA copper foil with 0.4 mm thickness), BS1 (45° SA steel foil with 0.3 mm thickness), and BS5 (45° SA steel foil with 0.3 mm thickness) foil combinations. Similar observations were made

Fig. 8 Load capability of GFTB with steel foils (Table 1)
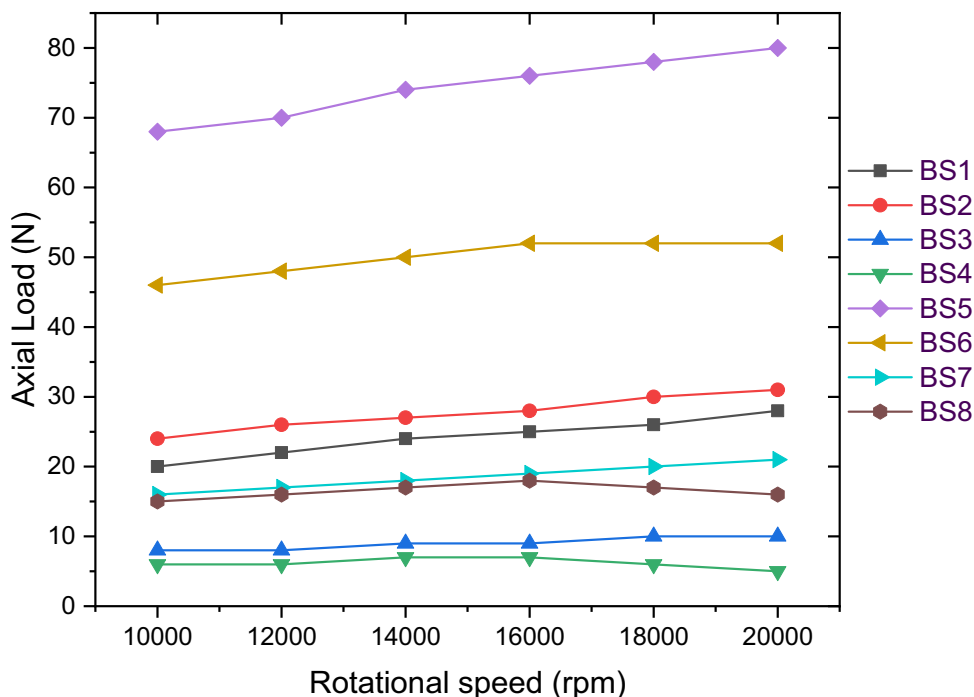
Fig. 9 Load capability of GFTB with copper foils (Table 2)
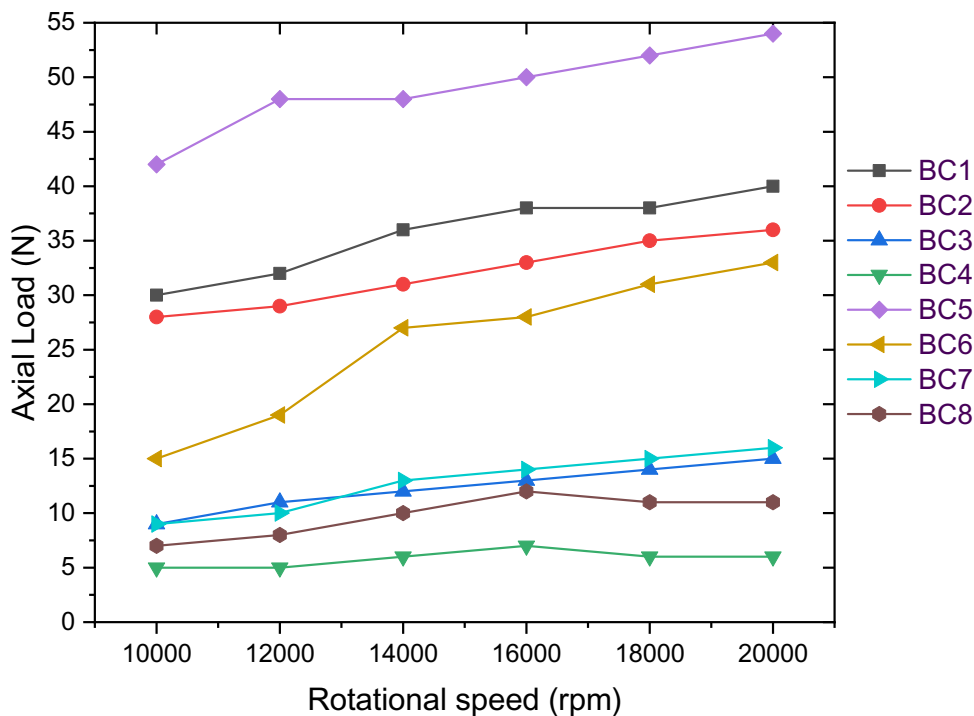
with three and six foils for FTB with BC2 (45° SA copper foil with 0.3 mm thickness), BC6 (45° SA copper foil with 0.4 mm thickness), BS2 (45° SA steel foil with 0.3 mm thickness), and BS6 (45° SA steel foil with 0.3 mm thickness) foil combinations as plotted in Fig. 11.

3.3 Frictional torque

The torque due to friction of the FTB termed as frictional torque or drag torque is determined experimentally for all the foil configurations. The frictional force (N) (or) tangential
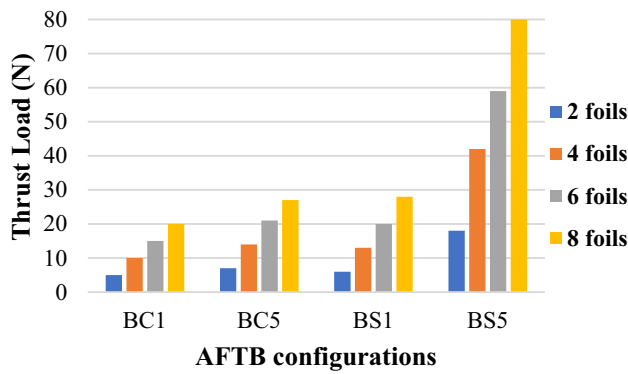
Fig. 10 Thrust loads versus GFTB with 45° angular foils
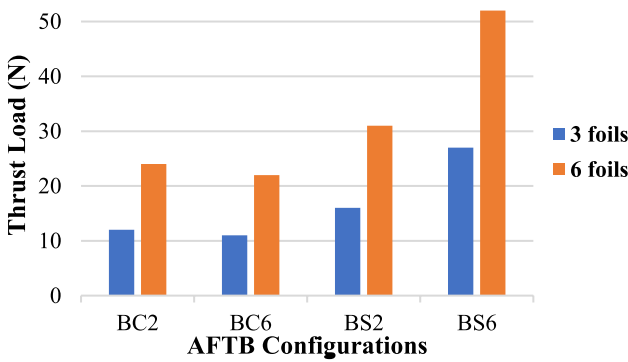
**Fig. 11** Thrust loads versus GFTB with 60° angular foils
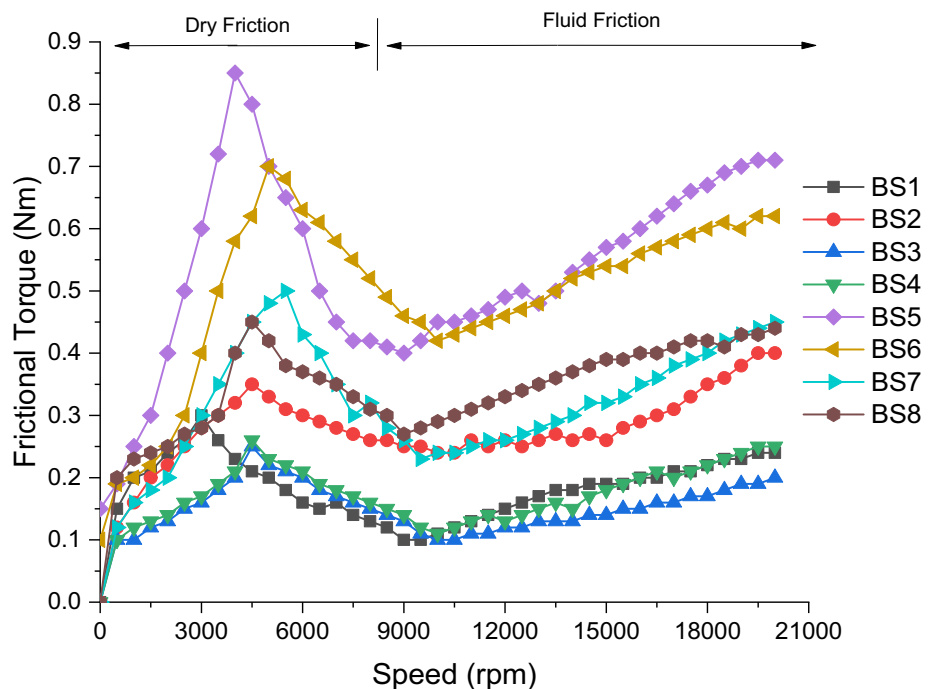
load acting on the bearing pad measured by means of a load cell is multiplied to the radial distance (m) between the centre of bearing and the load point gives the frictional torque (Nm). The drag torque readings for an AFTB are obtained for all the operating speeds with an interval of 500 rpm. Initially the foil rubs over the surface of the thrust runner up to its lift-off speed that forms a dry friction region and later the foil deflects back as the speed rises forming a fluid (air) friction region. The drag torque rises up to a peak point (due to foil wear) and subsequently decreases (due to foil deflection) in the dry friction range, eventually the torque rises at higher speeds in the fluid friction region. Figures 12, 13 shows the plot of the obtained frictional toque for all operating speeds for an AFTB with steel and copper foils respectively following almost similar trend of slopes. The BS5 (heat treated steel foil configuration) GFTB exhibited higher dry friction torque of about 0.85 Nm with 4,400 rpm being its lift-off speed. The frictional torque slope of all the AFTB foil configuration, increased with increase in operating speeds in both steel and copper heat-treated foils. The BS5 and BC5 bearing had higher drag torque at higher speeds, since they supported higher loads due to larger number of 45° sector angled foils. The drag torque (Nm) multiplied with the angular velocity (in terms of rad/sec) calculates the power losses of the FTB (in terms of Watts) for all the foil configuration of AFTB. The power losses of BS1 to BS8 bearings and BC1 to BC8 bearings are plotted in Figs. 14, 15 respectively. The slope indicates that the power loss is higher at higher operating speeds for those bearing configuration that supported larger thrust loads. This depicts that the dynamic thrust load (or dynamic structural stiffness) of any foil bearing at any

Fig. 12 Drag torque of GFTB with steel foils for all operating speeds (Table 1)

Fig. 13 Drag torque of GFTB with copper foils for all operating speeds (Table 2)
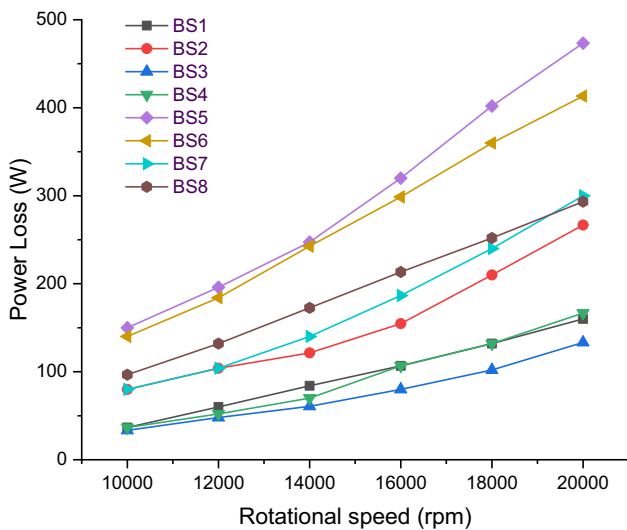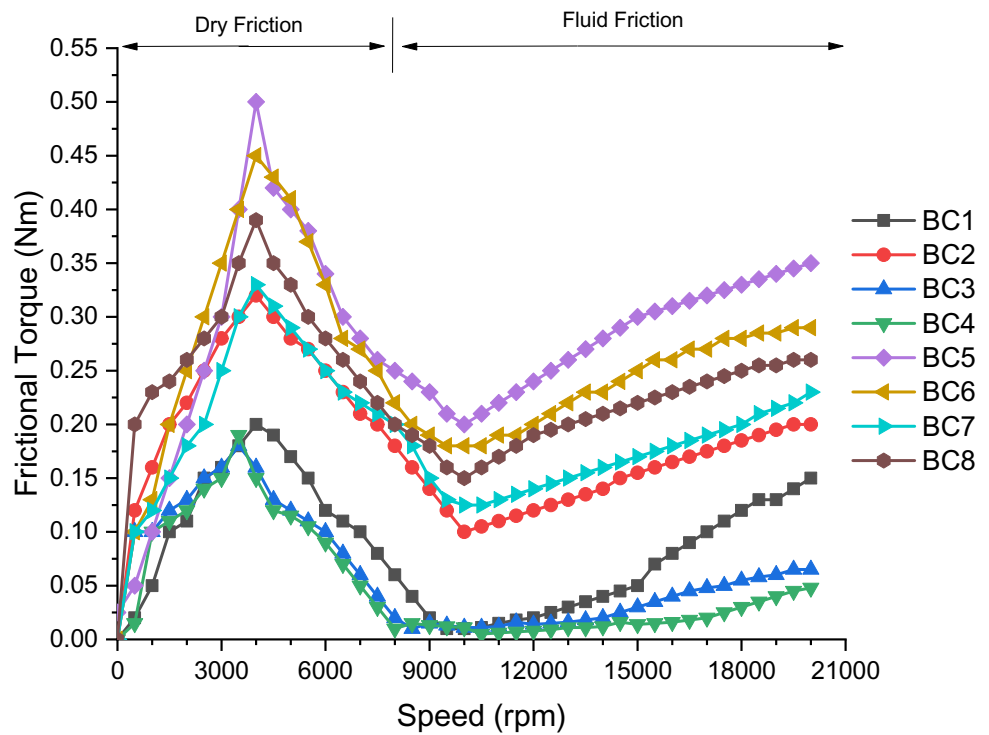
**Fig. 14** Power losses of various configurations of AFTB (Table 1)
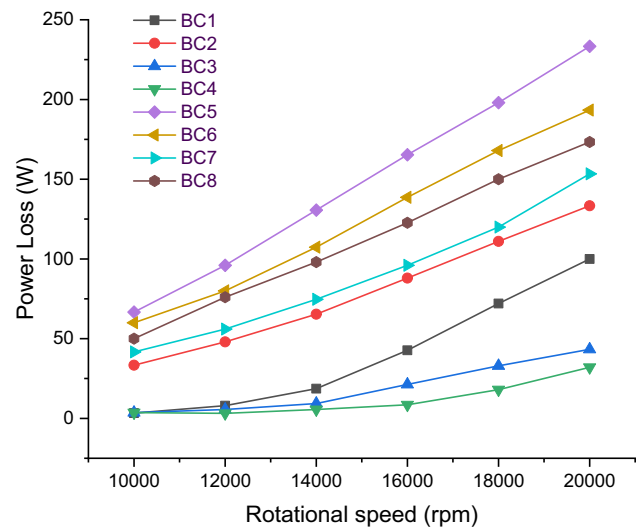
Fig. 15 Power losses of various configurations of AFTB (Table 2)

operating speed is directly proportional to the drag torque following the power loss.

3.4 Temperature

The temperatures characteristics of the AFTB are established using four precise k-type thermocouples positioned just beneath the upper foils attached to the bearing pad or plate, which records the temperatures. The test rig displays the average temperature from all the thermocouples in degree Celsius for each FTB foil configuration. The temperature values of all the bearings with steel and copper foil combinations for various operating speeds (10,000 rpm to 20,000 rpm) are as plotted in Figs. 16, 17. It was observed that the bearing temperature of a BS5 FTB is about 60 °C while that of a BC5 FTB is about 47 °C at 20,000 rpm. The foil bearing temperature (almost same as that of the fluid or air) increases with increase in operating speeds due to
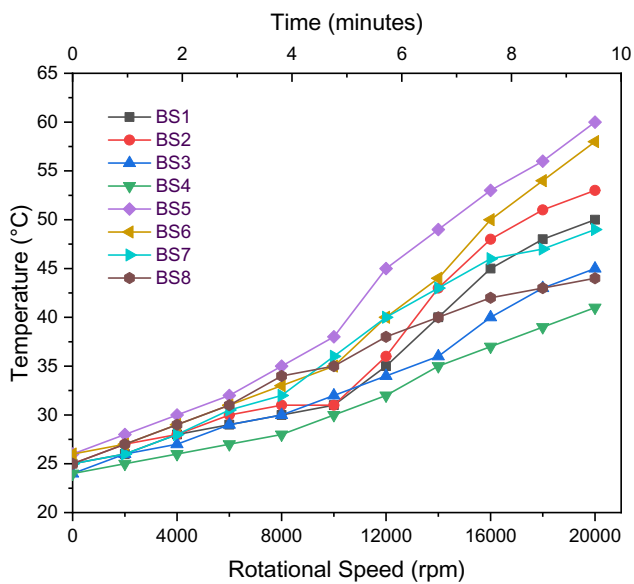
Fig. 16 Temperatures of AFTB with steel foil configurations (Table 1)
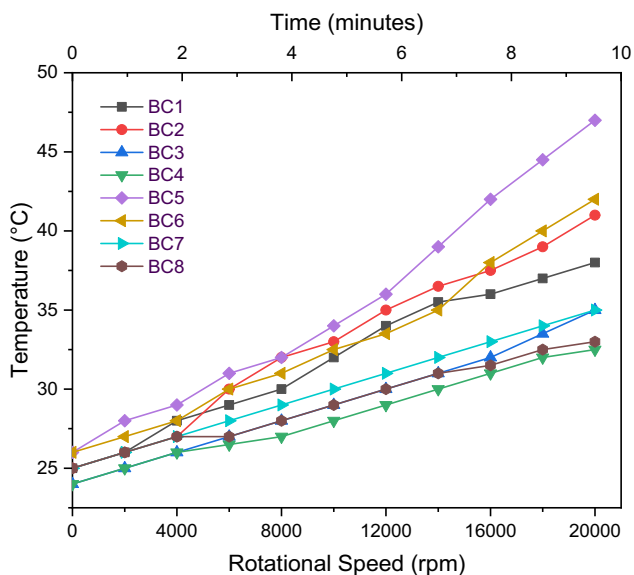
Fig. 17 Temperatures of AFTB with copper foil configurations (Table 2)

higher velocity of the fluid. Also, the density of the working medium (air) of the FTB decreases and the fluid becomes high viscous that intern carries higher thrust loads. Observations revealed that the temperatures for all FTB configurations rose as the dynamic measuring time increased, reaching a steady state after a specific duration (approximately 10 min in this case). AFTB with heat-treated copper foils exhibited lower temperatures, due to its lower load-bearing capability when compared to that of the heat-treated steel

foils. The numerical values of all the tests depicted in these graphs are the average results from three experimental trials conducted for each thrust foil bearing configuration. Meticulous observations were made when recording values from the calibrated test rig, both before and after the experiments.

4 Concluding remarks

The parametric study involved in the present work deals in development of an AFTB for a larger diameter (224 mm) capable of operating up to 20,000 rpm speeds, by optimizing the number of foils, foil thickness, and sector angle for two foil materials. Design, fabrication, and testing of air foil bearings with sixteen sets of heat-treated foil configurations on a novel bearing unit are being presented, besides the measurement of static stiffness, dynamic thrust loads, drag torque, power loss, and bearing temperatures of GFTB at various speeds. The following are some of the primary conclusions from the current experimental study in terms of developing a finest GFTB that sustains greater thrust loads:

- The foil stiffness, in terms of foil geometry and foil thickness, primarily determines the static structural stiffness of the FTB. The BS1, BS5, BC1, and BC5 exhibited higher static stiffness due to increase in foil numbers and decrease in foil sector angles.
- The FTB experiences elevated dynamic axial loads at higher operating speeds, correlating with an augmentation in foil thickness for both steel and copper foils, although up to an optimal level. The FTB with BS5 foil combination carried larger axial load of about 80 N operated at 20,000 rpm speeds and thereby being applicable in turbocharges with lower speeds.
- In all rotating speeds, lower sector-angled foils with larger wedge surface area supported higher thrust loads for both foil materials having 0.4 mm foil thickness. Additionally, FTB supported larger loads linearly with increment in number of foils on the bearing pad.
- The frictional torque and in-turn power loss of an AFTB is directly proportional to thrust loads and operating speeds of the foil bearing. The measured temperature of each AFTB increases with increase in operating speeds and load bearing capacity of foil thrust bearing.

Experimental studies on possible enhancement of FTB loads based on varying design parameters such as foil inclination angle together with foil sector angles for both the foil materials are the future scope of this research. The possibilities of continuous research include the testing of GFTB at operating speeds higher than 20,000 rpm along with the reduction of wear at start-stop cycles.

Data availability The authors confirm that the data supporting the findings of this study are available upon request.

Declarations

Conflict of interest The authors declare that they have no known competing financial interests or personal relationships that could have appeared to influence the work reported in this paper.

References

1. Agrawal GL (1997) Foil air/gas bearing technology—an overview. Turbo Expo: Power for Land, Sea, and Air 2(78682):0014006. https://doi.org/10.1115/97-GT-347
2. Heshmat H, Hermel P (1993) Compliant foil bearings technology and their application to high speed turbomachinery. Tribol Ser 25:559–575. https://doi.org/10.1016/S0167-8922(08)70411-5
3. Shivakumar S, NagaRaju T, Ravikumar RN, Rudraiah MC (2022) A review on performance characteristics of an air foil thrust bearing. Tribol Online 17(4):276–282. https://doi.org/10.2474/trol.17.276
4. Yong-Bok L, Tae YK, Chang HK, Tae HK (2011) Thrust Bump air Foil bearings with variable axial load: theoretical predictions and experiments. Tribol Trans 54(6):902–910. https://doi.org/10.1080/10402004.2011.606957
5. Kikuchi H, Ibrahim MD, Ochiai M (2019) Evaluation of lubrication performance of foil bearings with new texturing. Tribol Online 14(5):339–344. https://doi.org/10.2474/trol.14.339
6. Kim TH, Lee YB, Kim TY, Jeong KH (2012) Rotordynamic performance of an oil-free turbo blower focusing on load capacity of gas foil thrust bearings. J Eng Gas Turbines Power 134(2):1–7. https://doi.org/10.1115/1.4004143
7. Lee YB, Park DJ, Kim TH, Sim K (2012) Development and performance measurement of oil-free turbocharger supported on gas foil bearings. J Eng Gas Turbines Power 134:32506. https://doi.org/10.1115/1.4004719
8. Shi T, Huang H, Chen Q, Peng X, Feng J (2022) Performance investigation and feasibility study of novel gas foil thrust bearing for hydrogen fuel cell vehicles. Int J Energy Res 46(9):12642–12659. https://doi.org/10.1002/er.8033
9. Liu X, Li C, Du J, Nan G (2021) Thermal characteristics study of the bump foil thrust gas bearing. Appl Sci 11(9):4311
10. Guo Y, Hou Y, Zhao Q, Ren X, Chen S, Lai T (2022) Numerical and experimental studies on the thermal and static characteristics of multi-leaf foil thrust bearing. Proc Inst Mech Eng Part J J Eng Tribol 236(3):405–420. https://doi.org/10.1177/13506501211011019
11. Chen RG, Zhou Q, Liu Y, Hou Y (2011) A preliminary study of the load bearing capacity of a new foil thrust gas bearing. Proc Inst Mech Eng, Part C J Mech Eng Sci 225(3):673–678. https://doi.org/10.1243/09544062JMES2426
12. Zhou Q, Hou Y, Chen R (2012) Development of foil thrust bearings with simple structure for micro turbines. Adv Mater Res 368–373:1392–1395. https://doi.org/10.4028/www.scientific.net/AMR.368-373.1392
13. Dykas BEB (2009) Design, fabrication, and performance of foil gas thrust bearings for microturbomachinery applications. J Eng Gas Turbines Power 131:1–8. https://doi.org/10.1115/1.2966418
14. Kozanecki Z, Łagodziński J, Tkacz E, Miazga K (2018) Performance of thrust airfoil bearing for oil-free turbomachinery. J Vib Eng Technol 6(1):1–6. https://doi.org/10.1007/s42417-018-0001-z
15. Xu F, Chu J, Sha L (2022) Air foil thrust bearings with top foil sagging: theoretical predictions and experiments. Tribol Int 177:107995. https://doi.org/10.1016/j.triboint.2022.107995
16. Li C, Du J, Li J, Xu Z, Zhao C (2023) Investigations on the load capacity of multilayer foil thrust bearing based on an updated complete model. J Tribol 145(2):1–18. https://doi.org/10.1115/1.4055130
17. Ravikumar RN, Rathanraj KJ, Arun KV, Supreeth S (2023) Experimental and CFD analysis of a gas-lubricated foil thrust bearing for various foil configurations. FME Trans 51(4):532–540. https://doi.org/10.5937/fme2304532R
18. Ravikumar RN, Rathanraj KJ, Kumar VA (2016) Comparative experimental analysis of load carrying capability of air foil thrust bearing for different configuration of foil assembly. Proc Technol 25:1096–1105. https://doi.org/10.1016/j.protcy.2016.08.215
19. Supreeth S, Ravikumar RN, Raju TN, Dharshan K (2022) Foil stiffness optimization of a gas lubricated thrust foil bearing in enhancing load carrying capability. Mater Today Proc 52:1479–1487. https://doi.org/10.1016/j.matpr.2021.11.210
20. Supreeth S, Raju TN, Ravikuma RN, Mahesha CR (2023) Parametric studies on performance of oil-free thrust foil bearings at lower speeds. Tribol Ind 45(1):81–88. https://doi.org/10.24874/ti.1407.11.22.12
21. Hwang SH, Mehdi SM, Kim TH (2023) Static performance measurements and model predictions of gas foil thrust bearing with curved incline geometry. Lubricants 11(11):480. https://doi.org/10.3390/lubricants11110480
22. Hu B, Hou A, Deng R, Wang R, Wu Z, Ni Q, Li Z (2023) Numerical investigation of bump foil configurations effect on gas foil thrust bearing performance based on a thermos-elastic-hydrodynamic model. Lubricants 11(10):417. https://doi.org/10.3390/lubricants11100417
23. Tammineni NM, Mutra RR (2023) A review on recent advancements in an automotive turbocharger rotor system supported on the ball bearings, oil film and oil-free bearings. J Braz Soc Mech Sci Eng 45:481. https://doi.org/10.1007/s40430-023-04383-8